Decomposition of Nitrous Oxide on Rare Earth Manganites

S. LOUIS RAJ AND V. SRINIVASAN

Department of Chemistry, Indian Institute of Technology, Madras 600 036, India

Nitrous oxide decomposition was studied on a series of isostructural rare earth manganites of the general formula $LnMnO_3$ (where Ln = La, Nd, Sm or Gd) at an initial pressure of 200 Torr. Correlations of activation energies with lattice parameters suggest the importance of oxygen desorption as the rate determining step. The participation of the rare earth ion is discussed.

INTRODUCTION

Perovskite-type compounds derived from $LaMnO_3$ by the substitution of La^{3+} by other rare earth ions are well known (*1, 2*). The compound $LaMnO_3$ has been reported (*3*) to have an extensive nonstoichiometry inherently reaching up to the maximum of $LaMnO_{3.15}$, in contrast to other lanthanum transition metal perovskites $LaBO_3$ (B = transition metal ion). The electrical and magnetic properties of these compounds have been extensively studied and related to crystal structure and defect chemistry (*4*). These compounds have been found to have comparable catalytic activity for CO oxidation (*5*) and NO reduction (*6*).

The present study of the kinetics of the decomposition of nitrous oxide on a series of isostructural ternary oxides of the general formula $LnMnO_3$ (where Ln = La, Nd, Sm, or Gd) aims at (i) evaluation of the catalytic activities of these compounds for oxidation reactions and (ii) correlation of catalytic activity with lattice parameters. No detailed report is available of any previous study of this reaction over these manganites. Transition metal ions are active for this decomposition reaction. These ions have been dispersed isostructurally in the relatively inert and highly symmetrical oxides MgO, ZnO, and $MgAl_2O_4$ and the catalytic activity for this reaction has been investigated (*7, 8*). The compounds used in the present study contain the catalytically active Mn ion in oxygen octahedra linked by lanthanide ions in dodecahedral coordination.

MATERIALS AND METHODS

The rare earth manganites were prepared (*9*) by the coprecipitation of the rare earth ion and manganese ion from a mixture of their nitrate solutions using ammonium carbonate and firing the precipitate at 950°C in air. The formation of the perovskite phase was characterized by X-ray diffraction and chemical analysis. Since the percentage of the tetrapositive transition metal ion in rare earth manganites is dependent upon the firing temperature and ambient atmosphere, the compositions of Mn^{4+} in the samples were confirmed (*10*) by the analysis of the oxidizing power of the sample for the oxidation of Fe^{2+} to Fe^{3+} ($Mn^{3+}/Mn^{4+} \rightarrow Mn^{2+}$). The surface areas of the samples were determined by means of the BET method using nitrogen as the adsorbate. The physicochemical properties of the manganites are listed in Table 1.

The kinetics of the decomposition reaction were studied in a static recirculatory reactor of volume 160 ml. Nitrous oxide, at a pressure of 200 ± 1 Torr (1 Torr = 133 N m^{-2}), was admitted to the system. About 1.5 g of the catalyst was placed in the catalyst tube. The catalyst tube was heated by a furnace, the temperature of which was controlled to ± 1°C by a Sunvic energy regulator. The gases were circulated by means

TABLE 1

Physicochemical Characteristics of the Manganites

Catalyst	Surface area $(m^2 g^{-1})$	Percentage of Mn^{4+}	Oxidizing power
$LaMnO_3$	4.1	17.57	0.4861
$NdMnO_3$	5.4	17.65	0.4757
$SmMnO_3$	3.4	20.52	0.4758
$GdMnO_3$	2.9	18.42	0.4550

of a magnetic circulation pump. Catalytic activity was tested at several circulating speeds in order to make sure that mass transfer effects were not controlling the rate of the chemical reaction. The reaction rate was followed by noting the increase of pressure as a function of time using a traveling microscope of accuracy ±0.001 cm. After each kinetic run, the catalyst was evacuated at a final pressure of 10^{-6} Torr at 500°C for 6 hr. This procedure for surface restoration was found to give reproducible results. We point out that evacuation for 4 or for 8 hr at a final pressure of 10^{-6} Torr did not in any way affect the kinetics, indicating that the surface is not being reduced during evacuation. Hence the catalyst was evacuated for 6 hr uniformly throughout the study.

RESULTS AND DISCUSSION

From the observed intensities and the calculated interplanar spacings of the X-ray diffraction patterns, the cell constants for the orthorhombic system were evaluated and are presented in Table 2. The order of lattice parameters $c/2^{1/2} < a < b$ characteristic of an orthorhombic system has been confirmed (11). For the $LaMnO_3$ prepared, the cell constants show little difference from the values reported in a previous work (12). This indicates that the compound is nonstoichiometric and the formula is $LaMnO_{3+\lambda}$. Chemical analysis showed the presence of Mn^{4+} up to a level of ≈20%. This gives the formula $LaMnO_{3+\lambda}$ ($\lambda \approx 0.1$). For $LaMnO_3$, this oxidative nonstoichiometry is well studied (13) and it has

been established that the volume per formula unit (V_f) of $LaMnO_{3+\lambda}$ decreases with increasing oxidation. The volume per formula unit, 59.45 $Å^3$, calculated for the $LaMnO_{3+\lambda}$ studied, agrees well with reported values (13) and accounts for $\lambda = 0.0875$, the value arrived at from chemical analysis of Mn^{4+} (17.57%).

This large nonstoichiometric behavior of $LaMnO_3$ in comparison with other compounds in the $LaBO_3$ transition metal series has been attributed (13) to the loss of the e_g antibonding electron responsible for Jahn Teller distortion, from Mn^{3+} on its oxidation to Mn^{4+}. This results in a large decrease in ionic radius from Mn^{3+} to Mn^{4+}. This reduction in ionic radius is much larger than that found for other transition metal ions (14). This oxidative nonstoichiometry, amounting to $\lambda \approx 0.1$, exists also in the other manganites reported in this paper.

The kinetics of the decomposition of nitrous oxide obey different rate equations depending upon the initial pressure (15). At an initial pressure of 200 Torr, the rate expression

$$- \frac{dP_{N_2O}}{dt} = \frac{kP_{N_2O}}{P_{O_2}^{1/2}} \qquad (1)$$

was found to suit the experimental data perfectly. This would imply that the rate of the reaction is strongly inhibited by oxygen. The experimental data were analyzed using the integrated form of the above equation,

$$\frac{P_0^{1/2}}{2^{1/2}} \ln \frac{P_0^{1/2} + X^{1/2}}{P_0^{1/2} - X^{1/2}} - 2^{1/2}X^{1/2} = kt, \qquad (2)$$

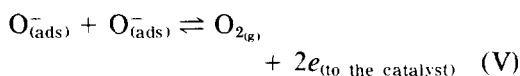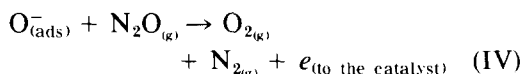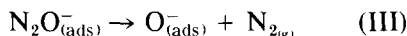where

TABLE 2

Cell Constants for an Orthorhombic System (Å)

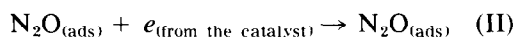| Catalyst	a	b	c	$c/2^{1/2}$
$LaMnO_3$	5.454	5.6539	7.7103	5.4460
$NdMnO_3$	5.3765	5.7059	7.5013	5.3160
$SmMnO_3$	5.3568	5.7940	7.4340	5.2670
$GdMnO_3$	5.3391	5.8028	7.3708	5.2150

P_0 is the initial pressure of nitrous oxide and

X is the pressure of nitrous oxide decomposed at the time t.

Plots of LHS (Eq. 2) vs time gave good straight lines even from the initial periods. This, taken in conjunction with our observation that very little oxygen is adsorbed on these catalysts, points to the fact that the nitrous oxide decomposition is stoichiometric. Typical kinetic plots are shown for $LaMnO_3$ in Fig. 1. The Arrhenius plots for the manganites are shown in Fig. 2. The specific reaction rate constants, apparent activation energies, and frequency factors are presented in Table 3.

The general mechanism proposed for nitrous oxide decomposition on metal oxides (16) is shown below.

$$N_2O_{(g)} \rightleftharpoons N_2O_{(ads)} \quad (I)$$

$$N_2O_{(ads)} + e_{(from\ the\ catalyst)} \rightarrow N_2O^-_{(ads)} \quad (II)$$

$$N_2O^-_{(ads)} \rightarrow O^-_{(ads)} + N_{2(g)} \quad (III)$$

$$O^-_{(ads)} + N_2O_{(g)} \rightarrow O_{2(g)}$$
$$+ N_{2(g)} + e_{(to\ the\ catalyst)} \quad (IV)$$

FIG. 1. Typical kinetic plots for $LaMnO_3$.

FIG. 2. Arrhenius plots for the manganites.

$$O^-_{(ads)} + O^-_{(ads)} \rightleftharpoons O_{2(g)}$$
$$+ 2e_{(to\ the\ catalyst)} \quad (V)$$
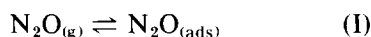
Generally in perovskites, the A ions are catalytically inactive and the active transition metal ions are placed at sufficiently large distances from each other (4 Å) so that a gas molecule interacts with a single site (9).

It has been observed that the kinetics of N_2O decomposition could be satisfactorily fitted into Eq. (1) which implies a negative half-order dependence on oxygen partial pressure. The isotopic oxygen exchanges studied by Sazonov et al. (17) on $LaBO_3$ oxides (where B is a transition metal ion) and by Winter (18) on a number of oxides have shown that there is complete correspondence between the kinetic parameters observed for the isotopic oxygen exchange and N_2O decomposition on the same catalysts. In the isotopic oxygen exchange reaction, it has been unequivocally established that the oxygen desorption step

$$2(^{16}O^-/\square s^-) \rightleftharpoons {}^{16}O_{2(g)} + 2\square s^- + 2e$$
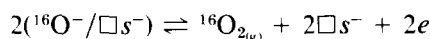
(similar to step (V) in the N_2O decomposition reaction mechanism) is rate controlling. Winter has also shown the possibility

TABLE 3

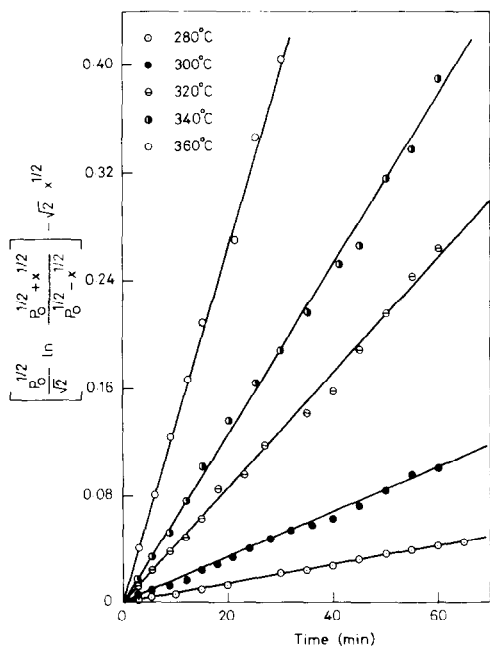Kinetic Parameters for N_2O Decomposition on $LnMnO_3$ Oxides
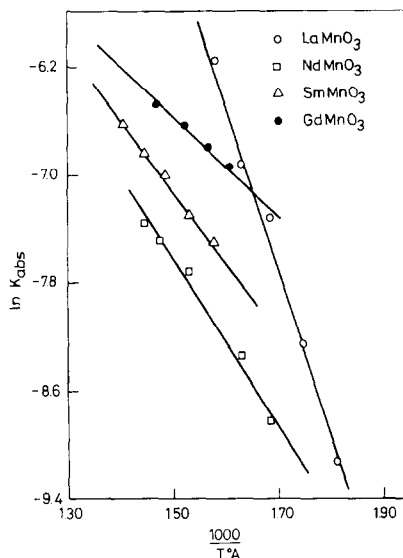
Catalyst	Temperature (°C)	Rate constant ($mm^{1/2}$ min^{-1} m^{-2})	E_a (kcal $mole^{-1})^a$	$\ln A$
$LaMnO_3$	280	1.009×10^{-4}	25.42	14.157
	300	2.600×10^{-4}		
	320	6.618×10^{-4}		
	340	9.882×10^{-4}		
	360	2.132×10^{-3}		
$NdMnO_3$	320	1.485×10^{-4}	12.42	1.830
	340	2.365×10^{-4}		
	380	4.428×10^{-4}		
	405	5.620×10^{-4}		
	410	6.331×10^{-4}		
$SmMnO_3$	360	5.454×10^{-4}	9.90	0.385
	380	6.817×10^{-4}		
	400	9.296×10^{-4}		
	420	1.060×10^{-3}		
	440	1.325×10^{-4}		
$GdMnO_3$	350	9.653×10^{-4}	6.46	-1.695
	365	1.113×10^{-3}		
	385	1.306×10^{-3}		
	410	1.531×10^{-3}		

^{a} 1 kcal = 4184 J.

of critical O–O distance deciding the efficiency of the catalyst. It can be similarly argued that in our present studies, the decomposition of N_2O should predominantly involve the desorption of oxygen as the rate-determining step.

Plots of activation energy for N_2O decomposition vs the cell constants along the a axis and the c axis are shown in Fig. 3. It is seen that a linear relationship is obtained indicating the increase of activation energy with the increase of the cell constant. Wolfram et al. have shown (19) the Mn or Mn–O–Mn group to be the active site in these manganites. The (100) face of perovskites containing a Mn–O–Mn square array has been shown (20) to be the most stable face. It may therefore be inferred in the present study also that the (100) face containing the Mn–O–Mn group is active for decomposition. When the cell constant increases, the Mn–O bond length increases, thereby weakening the Mn–O bond and increasing

the d electron density around the Mn ion. This would result in a strong interaction between the transition metal ion and the adsorbed oxygen. At 200 Torr N_2O pressure, the surface of the catalyst can be
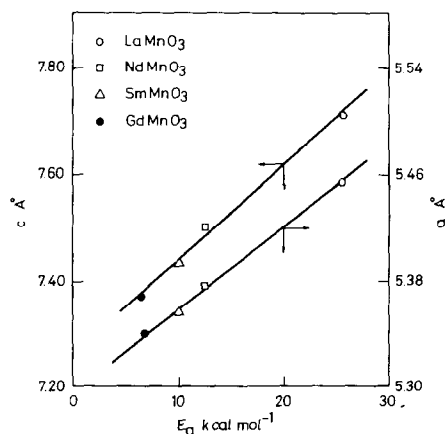

FIG. 3. Plots of activation energy for N_2O decomposition vs the cell constants along the a axis and the c axis.

expected to be saturated with N_2O so that the surface migration of oxygen (step (V) in the reaction mechanism) and its desorption would become difficult. An increase in the cell constant also increases the distance between two adjacent Mn ions, making the process of getting two O^- ions near enough to each other to desorb as O_2 comparatively difficult. From the above arguments, it is evident that the desorption of oxygen should be the rate-determining step in the decomposition reaction.

The decomposition of nitrous oxide has been shown (21) to be a suprafacial reaction, where the catalyst enters into the reaction as a relatively inert template providing a collection of atomic orbitals of proper symmetry and energy. The relevant energy levels are those around the Fermi level, i.e., the lowest unoccupied and the highest occupied levels. In the case of these manganites, the electronic structure is mainly dependent on the $3d$ levels of Mn ions and the p orbitals of oxygen. The Mn ions have to provide the empty d orbitals of suitable symmetry to overlap with filled p orbitals of oxygen (for electron transfer) in the desorption step. For Mn, these orbitals are the d_z2 and $d_{x2-y}2$. As one proceeds from lanthanum to gadolinium, the f electrons are being filled up successively and therefore one can expect a relative increase in the net electron density at the Mn ion sites, resulting in an increased occupancy at the e_g orbitals of Mn. As a result of this increased occupancy, the residual time of O^- on the Mn sites can be expected to decrease and the desorption to become more facilitated. This is reflected in the decrease of activation energy (Table 3) from La to Gd.

A plot of activation energy vs the logarithm of frequency factor is shown in Fig. 4. This gives a linear correlation suggesting the operation of a compensation effect (22). This would mean that energetically different sites are involved in the decomposition reaction. Since the same transition metal ion (Mn) is the active component for the
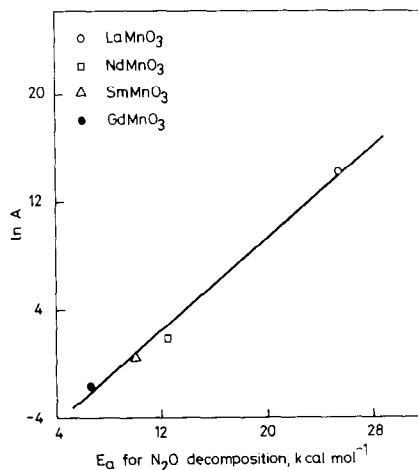

FIG. 4. A plot of activation energy vs the logarithm of the frequency factor.

reaction, energetically different sites of this ion are obviously possible only due to the variation of the rare earth ion. This would again confirm the participation of the rare earth ion in the decomposition reaction.

ACKNOWLEDGMENTS

REFERENCES

1. Jonker, G. H., and Van Santen, J. H., *Physica* **16**, 337 (1950).
2. McCarthy, G. J., Gallagher, P. V., and Sipe, C., *Mater. Res. Bull.* **8**, 1277 (1973).
3. Wold, A., and Arnott, R. J., *J. Phys. Chem. Solids* **9**, 176 (1959).
4. Elemans, J. B. A. A., Van Laar, K. R., Van Der Veen, and Loopstra, B. O., *J. Solid State Chem.* **3**, 238 (1971).
5. Voorhoeve, R. J. H., Remeika, J. P., Freeland, P. E., and Mathias, B. T., *Science* **177**, 353 (1972).
6. Voorhoeve, R. J. H., Remeika, J. P., and Johnson, D. W., Jr., *Science* **180**, 62 (1973).
7. Cimino, A., *Chem. Abstr.* **81**, 41859 C (1974).
8. Cimino, A., Indovina, V., Pepe, F., and Schiavello, M., *J. Catal.* **14**, 49 (1969).
9. Voorhoeve, R. J. H., Johnson, D. W., Jr., Remeika, J. P., and Gallagher, P. K., *Science* **195**, 827 (1977).
10. Bloom, E., Jr., Kometani, T. K., and Mitchell, J. W., *J. Inorg. Nucl. Chem.* **40**, 403 (1978).
11. Goodenough, J. B., and Longo, in "Landolt–

Bornstein Numerical Data and Functional Data in Science and Technology, New Series, Group III," Vol. 4a, p. 131. Springer-Verlag, New York, 1970.

12. Kamata, K., Nakajima, T., Hayashi, T., and Nakamura, T., *Mater. Res. Bull.* **13,** 49 (1978).

13. Tofield, B. C., and Scott, W. R., *J. Solid State Chem.* **10,** 183 (1970).

14. Shannon, R. D., and Prewitt, C. T., *Acta Crystallogr. B* **25,** 925 (1969); **26,** 1046 (1970).

15. Cimino, A., Indovina, V., Pepe, F., and Stone, F. S., *Gazz. Chim. Ital.* **103,** 935 (1973).

16. Winter, E. R. S., *J. Catal.* **15,** 144 (1969).

17. Sazonov, L. A., Mosvina, Z. V., and Artamonov, E. V., *Kinet. Katal.* **15,** 120 (1974).

18. Winter, E. R. S., *J. Catal.* **19,** 32 (1970).

19. Wolfram, T., Kraut, E. A., and Morin, F. J., *Phys. Rev. B* **7,** 1677 (1973).

20. Ahmed, L. I., *Surface Sci.* **12,** 437 (1968).

21. Voorhoeve, R. J. H., Remeika, J. P., and Trimble, L. E., *Ann. N. Y. Acad. Sci.* **272** (1976).

22. Galwey, A. K., *in* "Advances in Catalysis," Vol. 26, p. 247. Academic Press, New York, 1977.